Connecting Main-Group Metals (Al, Ga, In) and Tungsten(0) Carbonyls via the N_2S_2 Metallo-Ligand Strategy

Xuemei Yang, Allen Lunsford and Marcetta Y. Darensbourg *

Department of Chemistry, Texas A&M University, 3255 TAMU, College Station, TX 77843, USA; xuemeiyang@tamu.edu (X.Y.); allen.lunsford@intel.com (A.L.)
* Correspondence: marcetta@chem.tamu.edu; Tel.: +1-979-845-0158

Abstract: Tetradentate N_2S_2 ligands (such as bismercaptoethanediazacycloheptane in this study) have seen extensive use in combination with transition metals. Well-oriented N_2S_2 binding sites are ideal for d^8 transition metals with square planar preferences, especially Ni^{II}, but also as a square pyramidal base for those metals with pentacoordinate preferences, such as $[V{\equiv}O]^{2+}$, $[Fe(NO)]^{2+}$, and $[Co(NO)]^{2+}$. Further reactivity at the thiolate sulfurs generates diverse bi, tri, and tetra/heterometallic compounds. Few N_2S_2 ligands have been explored to investigate the possibility of binding to main group metals, especially group III (M^{III}) metals, and their utility as synthons for main group/transition metal bimetallic complexes. To open up this area of chemistry, we synthesized three new five-coordinate main group XMN_2S_2 complexes with methyl as the fifth binding ligand for M = Al, and chloride for M = Ga and In. The seven-membered diazacycle, dach, was engaged as a rigid stabilized connector between the terminal thiolate sulfurs. The pentacoordinate XMN_2S_2 complexes were characterized by ^{1}H-NMR, ^{13}C-NMR, $^+$ESI-Mass spectra, and X-ray diffraction. Their stabilities and reactivities were probed by adding Ni^{II} sources and $W(CO)_5(THF)$. The former replaces the main group metals in all cases in the N_2S_2 coordination environment, demonstrating the weak coordinate bonds of M^{III}–N/S. The reaction of XMN_2S_2 (XM = $ClGa^{III}$ or $ClIn^{III}$) with the labile ligand W(0) complex $W(CO)_5(THF)$ resulted in Ga/In–W bimetallic complexes with a thiolate S-bridge. The synthesis of XMN_2S_2 complexes provide examples of M^{III}–S coordination, especially Al–S, which is relatively rare. The bimetallic Ga/In–S–W complex formation indicates that the nucleophilic ability of sulfur is retained in M^{III}–S–R, resulting in the ability of main group M^{III}–N_2S_2 complexes to serve as metalloligands.

Keywords: N_2S_2 ligand; main Group III metals; gallium tungsten bimetallic

1. Introduction

In the early 1960s, Busch and co-workers reported the complexing ability of mercaptamines (NS ligands) for Ni^{II} [1]. Since then, various NS ligands have been reported, including those with a contiguous S–N–N–S, N_2S_2, tetradentate donor set, an arrangement that mimics the N_2S_2 coordination environment rendered by a cysteine-glycine/serine-cysteine tripeptide motif found at three enzyme active sites [2]. Further development has been robust. Of special note is the bimetallic Ni–Ni site in acetyl co-A synthase, ACS, in which N_2S_2 is viewed as a tight Ni-binding site, while the second nickel is labile and catalytically active in the C–C coupling reactions required of ACS, as shown in Figure 1 [3].
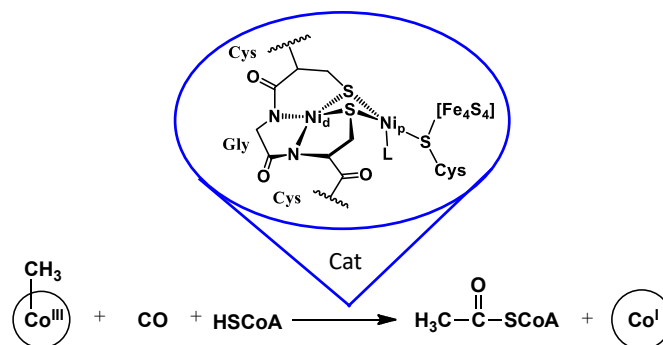
Figure 1. Structure and function of the dinickel enzyme active site of acetyl co-A synthase [3].

We developed NiN$_2$S$_2$ complexes as metallodithiolate ligands, especially engaging diazamesocycles N$_2$C$_6$H$_8$ (daco), N$_2$C$_5$H$_{10}$ (dach), and N$_2$C$_4$H$_8$ (dach*) as stabilizing units in N to N connections [4–6]. Those containing the more flexible "open-chain" ethylene or propylene N to N linkers bring more flexibility to the N$_2$S$_2$ binding unit, resulting in subtle differences in reactivity and stability properties. The ability to tune the MN$_2$S$_2$ ligands by variations of M has resulted in a range of complexes, such as V^{4+} in [V≡O]$^{2+}$, Fe^{2+} in {Fe(NO)}^{7}, Ni^{2+}, Pd^{2+}, Cu^{2+},and Zn^{2+} [7]. The ability of the MN$_2$S$_2$ metalloligands to serve as monodentate as well as bidentate ligands to a single metal or as bridging bidentate ligands to two metals has led to multiple new compositions and various diverse structural forms [7]. A few of these are illustrated in Figure 2 [7]. However, the chemistry of N$_2$S$_2$ derivatives of main group metals remains relatively unexplored, and their ability to serve as aggregation sites for exogeneous metals has until now, to our knowledge, been unreported.
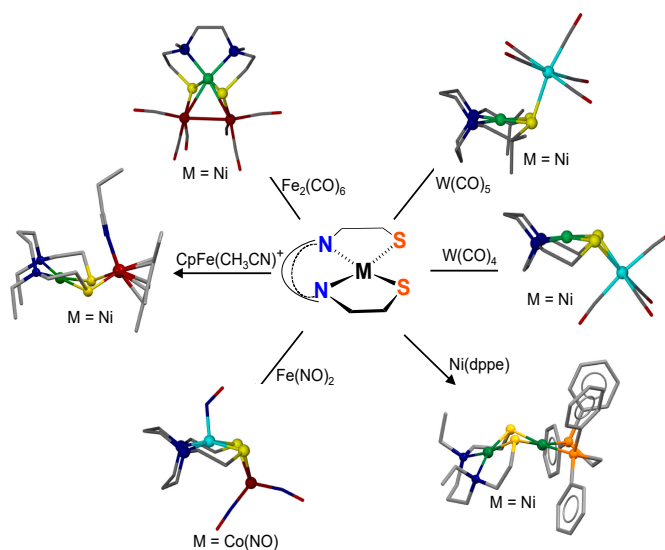

Figure 2. Examples of bi- and trimetallic complexes accessed by connecting the MN$_2$S$_2$ metallodithiolate ligand to various transition metal receivers, adapted from [7].

While the expectation that the soft S will have a poor binding affinity for hard Al(III) is reasonable, a Cambridge database search located 36 results of N$_2$S$_2$ derivatives of aluminum. Most of them are derived from an aluminum (I) precursor [8,9]. The use of abundant aluminum in catalysis is well known, including as catalysts for CO$_2$/epoxide cycloaddition [10,11], which comprises a tetradentate N$_2$O$_2$ ligand with an axial X ligand (X = alkyl, halogen completing the coordination sphere). In contrast, many more sulfur‑coordinated gallium(III) and indium(III) complexes have been reported, owing to the softer core of Ga(III)/In(III) [12–17]. Explorations in those cases have been prompted by the wide use of ^{111}In and ^{67}Ga as radionuclides in PET (Positron Emission Tomography) and SPECT (Single Photon Emission Computed Tomography) [18].

In order to extend the coordination chemistry of main group III metals with this versatile ligand motif, we explored the synthesis and characterization of Group III elements, such as Ga/In–Cl or Al–R, bound within the N_2S_2 binding cavity. We probed the availability of the residual S lone pairs to serve as nucleophiles for the binding to exogeneous metals. In particular, heterobimetallics were formed with $W(CO)_{4/5}$, a receiver unit with the CO reporter unit, which provides a reference point for establishing donor ability of such metalloligands [7].

2. Results

2.1. Synthesis and Characterizations of XMN_2S_2 Complexes

The H_2bme-dach (*N,N′*-Bis(Mercaptoethyl)-1,4-Diazacycloheptane) was synthesized according to a reported procedure [4]. Under an N_2 atmosphere, a solution of $AlMe_3$, $GaCl_3$, or $InCl_3$ was transferred by a double-ended needle into a solution of H_2bme-dach ligand in a Schlenk flask. White powdery products formed immediately, resulting in a white suspension. After stirring overnight, the solvent was removed under vacuum giving white solids, determined to be the compounds shown in Figure 3. They were further washed with Et_2O and pentane, giving a yield of 75–80%.
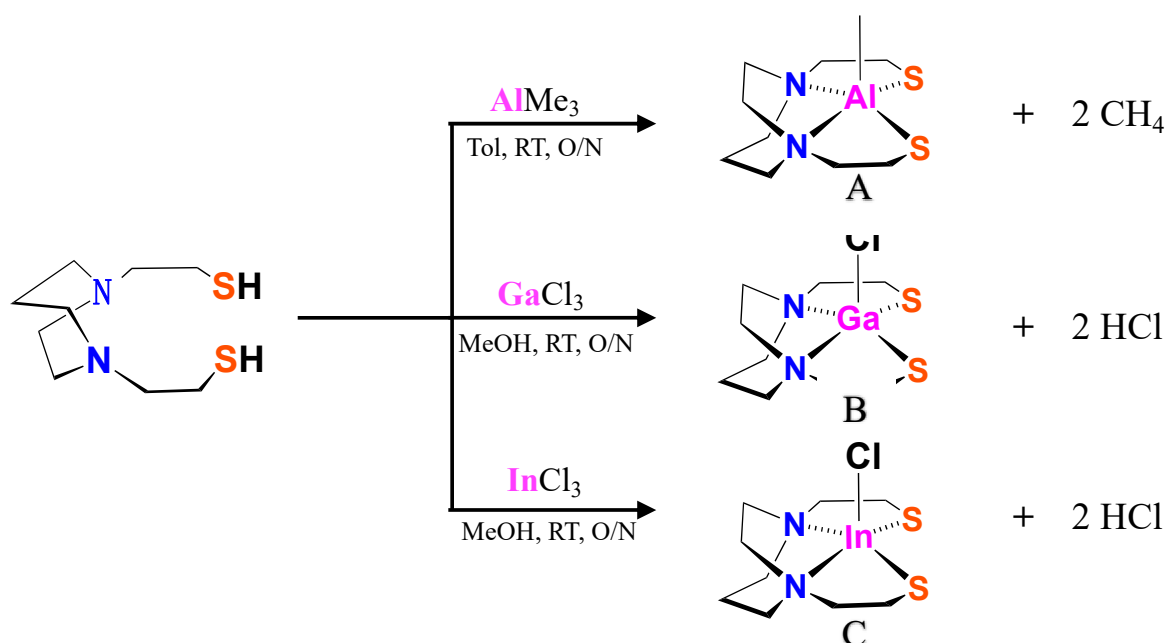

Figure 3. Synthetic routes for XMN_2S_2 complexes; RT is ca. 22 °C and O/N is ca. 14 h.

The XMN_2S_2 complexes were characterized by XRD, ESI-mass spectra, ^{1}H-NMR and ^{13}C-NMR. Details are shown in the Supporting Information. The X-ray quality crystals of **A** were developed in pyridine solution at −28 °C. Crystals of **B** and **C** were obtained by slow evaporation of Et_2O vapor into a pyridine solution. All crystals were colorless needles. Metric parameters for the molecular structures are given in Figure 4.
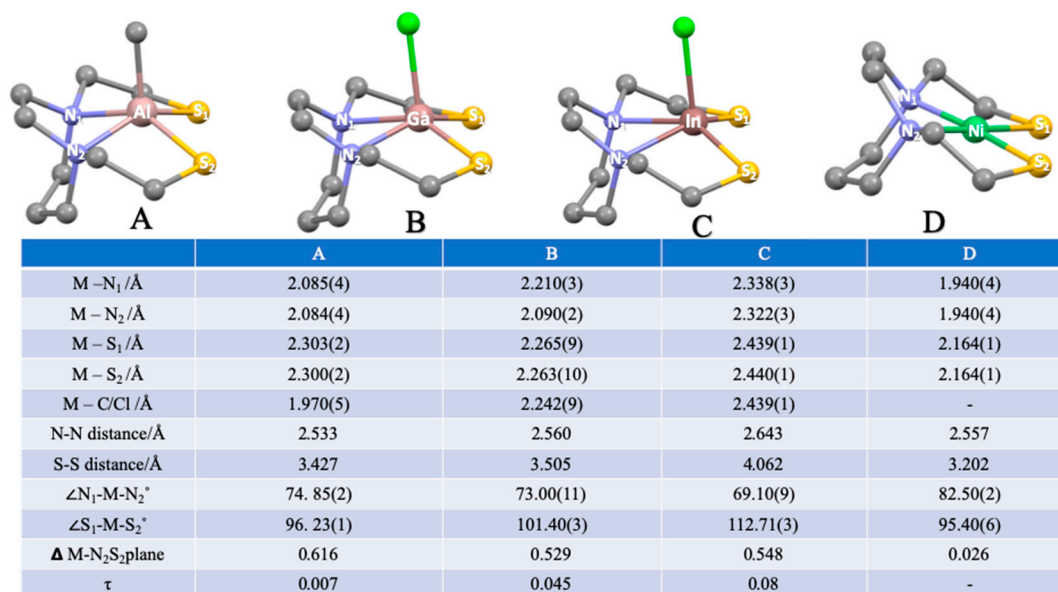
	A	B	C	D
$M-N_1$/Å	2.085(4)	2.210(3)	2.338(3)	1.940(4)
$M-N_2$/Å	2.084(4)	2.090(2)	2.322(3)	1.940(4)
$M-S_1$/Å	2.303(2)	2.265(9)	2.439(1)	2.164(1)
$M-S_2$/Å	2.300(2)	2.263(10)	2.440(1)	2.164(1)
M–C/Cl/Å	1.970(5)	2.242(9)	2.439(1)	-
N-N distance/Å	2.533	2.560	2.643	2.557
S-S distance/Å	3.427	3.505	4.062	3.202
$\angle N_1\text{-}M\text{-}N_2$°	74.85(2)	73.00(11)	69.10(9)	82.50(2)
$\angle S_1\text{-}M\text{-}S_2$°	96.23(1)	101.40(3)	112.71(3)	95.40(6)
Δ $M\text{-}N_2S_2$plane	0.616	0.529	0.548	0.026
τ	0.007	0.045	0.08	-

Figure 4. Molecular structures of XMN_2S_2 complexes from XRD analysis with selected metric data.

The geometries of XMN_2S_2 (M = Al, Ga, and In) were similar, as the ideality of the square pyramidal structures is indicated by small τ values (near 0) [19]. The displacements of M from the best N_2S_2 planes showed aluminum to be the most out of plane, Δ = 0.616 Å, while Ga and In showed displacements in the range of 0.53–0.55 Å. These displacements are likewise seen in some pentacoordinate transition metal complexes, such as MN_2S_2, where M = $[Co(NO)]^{2+}$ (0.31 Å), $[Fe(NO)]^{2+}$ (0.55 Å), and $[V\equiv O]^{2+}$ (0.652 Å) [20,21]. In all cases of **A**, **B**, and **C**, the two-carbon linker within the diazacycloheptane ring is on the same side as the M^{III}–X bond vector. This means that the MN_2C_3 cyclohexane-type ring in the chair configuration is oriented "underneath" the N_2S_2 base of the square pyramidal X–MN_2S_2 structure. We saw no evidence of fluxionality in the solution.

Different from Ga and In, which are largely located on the midpoint line in the center of the N_2S_2 unit, Al showed a slight dissymmetry in its location, shifted towards the nitrogen atoms (Al–N is around 2.1 Å) and away from the sulfur atoms (Al–S is around 2.3 Å). This suggests a stronger electrostatic interaction to N from the Al^{III}. Table S5 lists the comparative ratios of the M–N/M–S distances that emphasize the similarity of Ga and In and their greater affinity for sulfur. From Al, Ga, to In, the angles of ∠N–M–N decreased with a concomitant increase in ∠S–M–S.

2.2. Reactions of XMN_2S_2 with Ni(II) Sources

The optimal sized N_2S_2 cavity of the bme-dach and analogous ligands, as well as the electronic structure preference of d^8 Ni^{II}, leads to a well-known library of square planar NiN_2S_2 complexes [7]. Thus, we probed the possibility of Ni^{II} replacement of the Group III metal ions in the XMN_2S_2 complexes. Such metal exchange studies were not easily performed in the transition metal complexes, as aggregation at the sulfur elements was prominent.

The addition of $NiCl_2$ or $Ni(BF_4)_2$ to $XM^{III}N_2S_2$ complexes resulted in the formation of NiN_2S_2 with M^{III} replaced by Ni^{II}, concomitant with a color change from colorless to dark maroon, illustrated in Figure 5. The resulting maroon product gave a yield of 75–80% and was confirmed as the known NiN_2S_2 complex by mass spectroscopy (Figure S12) and X-ray structure analyses. To determine whether the XM^{III} unit might remain in the N_2S_2 cavity with the attachment of Ni(diphos) to the nucleophilic sulfurs of $XM^{III}N_2S_2$, we added the (diphos)$NiCl_2$ complex to a solution of $XM^{III}N_2S_2$. The product of that reaction was determined to be the well-known dinickel complex derived from two (diphos)$NiCl_2$ complexes with Ni^{II} moving into the tight binding site, replacing XM^{III}, and the second nickel holding on to the diphos ligand, Figure 5. The stability of the NiN_2S_2 complex relative to $XM^{III}N_2S_2$ was confirmed.
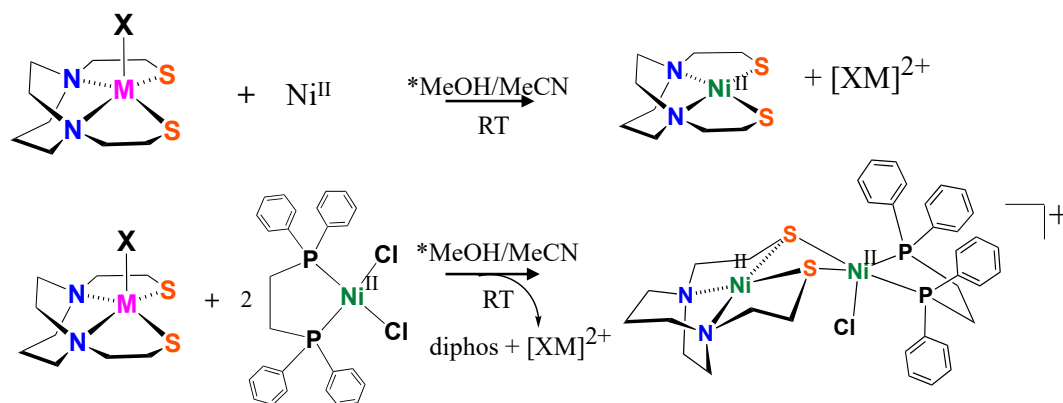
Figure 5. Reactions of XMN_2S_2 with Ni^{II} salts and (diphos)$NiCl_2$. * Pure MeOH, or MeCN, or a mixture of MeOH/MeCN (1:1) resulted in the same products.

2.3. Nucleophilicity of S Lone Pairs on XMN_2S_2 Towards the Soft Receiver $W(CO)_5$

The stability and electronic reporting capability of tungsten carbonyls have proven useful to rank the donor ability of various MN_2S_2 metalloligands. The labile ligand synthons $W(CO)_5$(solv) and $W(CO)_4$(solv)$_2$ were generated by appropriate methods [22,23]. Carbon monoxide was lost in solutions of $W(CO)_6$ in THF under UV light, after which the golden yellow solution showed the ν(CO) C_{4v} pattern typical of $W(CO)_5$(THF) and was transferred via cannula to a solution of XMN_2S_2 (XM = ClGa/ClIn). Over the course of several hours at room temperature, with no further photolysis, the color changed to brown-orange. As shown in the overlaid spectra in Figure 6, the shift in ν(CO) was not large, indicating the donor ability of THF and monodentate XMN_2S_2 toward $W(CO)_5$ is similar and weak. In contrast, NiN_2S_2 reacted with $W(CO)_5$(THF), producing a much greater change in ν(CO) of 2062 (w), 1922 (s), and 1884 (m) [23]. The $MeAlN_2S_2$ metalloligand itself is not stable under UV light and gave products of degradation in the presence of $W(CO)_5$(THF).
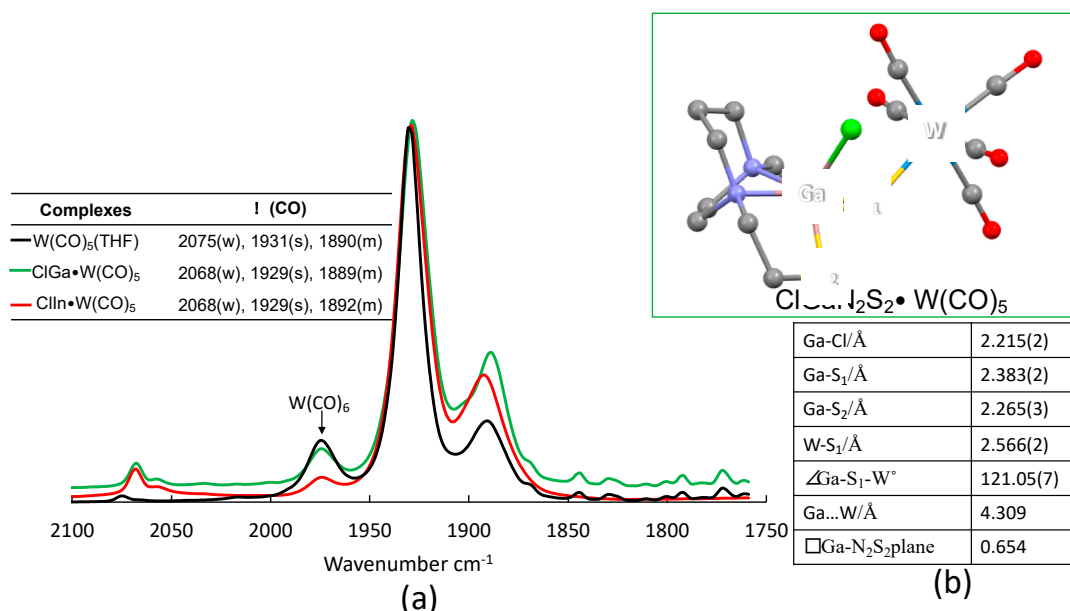

Complexes	ν(CO)
W(CO)$_5$(THF)	2075(w), 1931(s), 1890(m)
ClGa•W(CO)$_5$	2068(w), 1929(s), 1889(m)
ClIn•W(CO)$_5$	2068(w), 1929(s), 1892(m)

Ga-Cl/Å	2.215(2)
Ga-S$_1$/Å	2.383(2)
Ga-S$_2$/Å	2.265(3)
W-S$_1$/Å	2.566(2)
∡Ga-S$_1$-W°	121.05(7)
Ga...W/Å	4.309
☐Ga-N$_2$S$_2$plane	0.654

Figure 6. (**a**) IR spectra in ν(CO) region of products from reactions of $W(CO)_5$(THF) with XMN_2S_2; (**b**) XRD determined molecular structure of $ClGaN_2S_2 \cdot W(CO)_5$ with selected metric data.

Orange sheet crystals of $ClGaN_2S_2 \cdot W(CO)_5$ were obtained from THF solution by hexane layering. The X-ray diffraction study showed that the geometry and metric parameters were largely the same in the free and S-bound monodentate complexes. The Ga–S$_1$ bridge bond was elongated compared

with the $ClGaN_2S_2$ structure. The N_2S_2 "plane" was quite distorted, giving the $ClGaN_2S_2$ a geometry between square pyramidal and trigonal bipyramidal with the τ value 0.50, as shown in Figure S18 [19]. Gallium(III) was significantly more displaced from the N_2S_2 "plane", giving a deviation of over 0.1 Å (0.529 Å in $ClGaN_2S_2$ to 0.654 Å in $ClGaN_2S_2 \cdot W(CO)_5$). The distance between Ga and W was 4.309 Å.

On further exposing $ClGaN_2S_2 \cdot W(CO)_5$ to UV light, a second CO was lost, yielding $ClGaN_2S_2 \cdot W(CO)_4$. The $\nu(CO)$ IR spectrum displays a four-band pattern typical of C_{2v} metal carbonyl derivatives; the values are 2004 (w), 1929 (m), 1890 (m), and 1846 (m) cm^{-1} with the color changing to light orange, Figure 7. Similar to the $ClGaN_2S_2 \cdot W(CO)_5$ complex, the $ClInN_2S_2 \cdot W(CO)_5$ converted to $ClInN_2S_2 \cdot W(CO)_4$ under light, giving $\nu(CO)$ values of 2007 (w), 1929 (m), 1894 (m), and 1850 (m) cm^{-1}, as shown in Figure S17. The final product was confirmed by $^-$ESI-Mass, and details are given in the Supplementary Materials. The experimental results indicate that the thiolate sulfurs in the XMN_2S_2 complexes are still sufficiently active to bind another metal. However, the binding ability is weak. The latter statement was confirmed by the reversibility of the CO loss. On bubbling CO through the solution of $ClGaN_2S_2 \cdot W(CO)_4$, the pentacarbonyl was readily reclaimed.
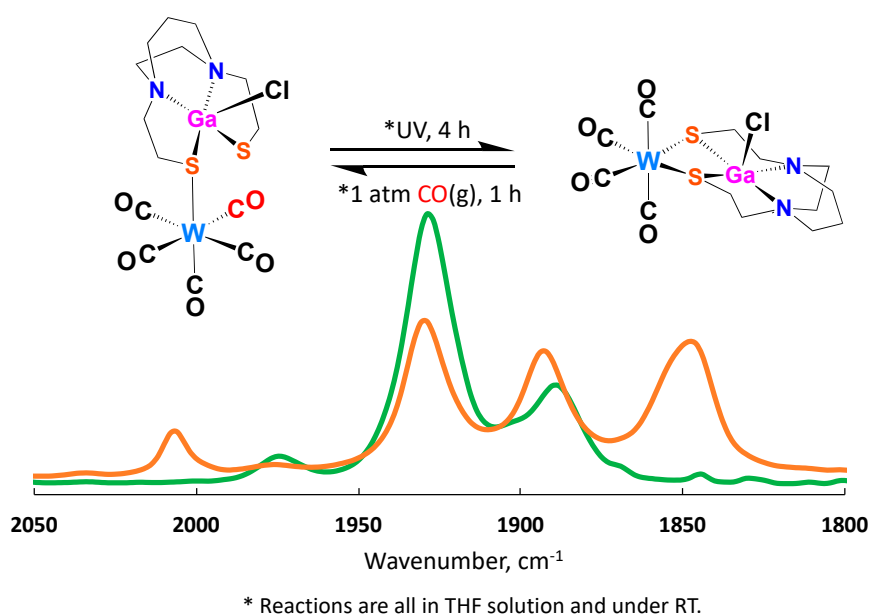
Figure 7. Reactions of $ClGaN_2S_2 \cdot W(CO)_5$ and $ClGaN_2S_2 \cdot W(CO)_4$ under UV light irradiation. $ClGaN_2S_2 \cdot W(CO)_5$ converted to $ClGaN_2S_2 \cdot W(CO)_4$ and, reversibility established by bubbling CO(g) to $ClGaN_2S_2 \cdot W(CO)_4$ resulting in the reformation of $ClGaN_2S_2 \cdot W(CO)_5$. The green line is for $ClGaN_2S_2 \cdot W(CO)_5$ and the orange line is for $ClGaN_2S_2 \cdot W(CO)_4$.

3. Materials and Methods

All reagents and solvents were obtained from commercial sources. All solvents were purified and dried by an MBRAUN Manual Solvent Purification System (MBRAUN, NH, USA) packed with Alcoa F200 activated alumina desiccant. All reactions and operations were carried out on a double manifold Schlenk vacuum line or in a glovebox under a N_2 or Ar atmosphere.

Solution infrared spectra were recorded on a Bruker Tensor 37 Fourier transform IR (FTIR) spectrometer (Billerica, MA, USA) using a CaF_2 cell with a 0.2 mm path length. Both High Resolution and Low Resolution Mass spectrometry (Thermo Fisher Q Exactive Mass Spectrometer, ESI-MS, (IET, IL, USA) were performed in the Laboratory for Biological Mass Spectrometry at Texas A&M University. Data collections for X-ray structure-determination were carried out using Bruker APEX2 (Billerica, MA, USA) or Venture with a graphite monochromated radiation source ($\lambda = 0.71073$ Å). All crystals were coated in paraffin oil and mounted on a nylon loop and placed under streaming N_2 (110/150K). The structures were solved by direct methods (SHELXS-97) and refined by standard Fourier techniques against F square with a full-matrix least-squares algorithm using SHELXL-97

and the WinGX (1.80.05) software package (University Of Glasgow, Scotland, UK). Hydrogen atoms were placed in calculated positions and refined with a riding model. Graphical representations were prepared with ORTEP-III. Crystallographic data (including structure factors) have been deposited with the Cambridge Crystallographic Data Centre as supplementary publication nos. 1943010–1943013.

3.1. Synthesis of XMN_2S_2

$MeAlN_2S_2$: The H_2bme-dach ligand (0.22 g, 1.0 mmol) was added to a 125 mL Schlenk flask by pipet in an inert atmosphere glove box and dissolved in ca. 10 mL toluene. A pentane solution of $AlMe_3$ (1 M in pentane, 1 mL, 1 mmol) was added dropwise to the ligand solution. After reacting overnight at room temperature, the resulting powdery white solution was filtered, and solvent was removed under vacuum. The white solid was washed with Et_2O and pentane, giving a ~75% yield. Proton NMR spectral values (300 MHz, 293 K, pyridine-d_5) were as follows: δ (ppm) = 4.98 (s, 8H, N_2S_2) 2.63(q, 2H, N_2S_2), 2.61(q, 8H, N_2S_2), 1.70(q, 2H, N_2S_2), 0.10(s, 1H, Me). ^{13}C NMR (300 MHz, 293 K, pyridine-d_5): δ (ppm) = 61.40, 55.80, 54.39, 28.81, 23.69, −4.01. High Resolution $^+$ESI-Mass: $[M + H]^+$ ($C_{10}H_{22}AlN_2S_2$) Calculated 261.1040 (Most Abundant Isotopic Mass); Found: 261.1033. The detailed isotope abundance is shown in Figure S4.

$ClGaN_2S_2$: Similar to $MeAlN_2S_2$, $ClGaN_2S_2$ was derived from a MeOH solution of $GaCl_3$ (0.176 g, 1.0 mmol) and H_2bme-dach (0.22 g, 1.0 mmol) at room temperature. After overnight reaction, the solvent was removed from the resulting powdery white suspension under vacuum, and the white solid was washed with Et_2O and pentane, giving an ~80% yield. ^{1}H NMR (300 MHz, 293 K, pyridine-d_5): δ (ppm) = 5.75(s, 8H, N_2S_2), 3.62(s, 4H, N_2S_2), 2.84(s, 2H, N_2S_2), 2.17(q, 2H, N_2S_2), 1.27(q, 2H, N_2S_2). ^{13}C NMR (300 MHz, 293 K, pyridine-d_5): δ (ppm) = 55.96, 51.54, 48.71, 24.62, 22.18. High Resolution $^+$ESI-Mass: $[M − Cl]^+$ ($C_9H_{18}GaN_2S_2$) Calculated 287.0162; Found: 287.0157 (Most Abundant Isotopic Mass). The detailed isotope abundance is shown in Figure S5.

$ClInN_2S_2$: $ClInN_2S_2$ was synthesized in a similar method to $ClGaN_2S_2$. A MeOH solution of $InCl_3$ (0.221 g, 1.0 mmol) was added dropwise to a MeOH solution of H_2bme-dach. The powdery suspension was dried, and the white solid was washed with Et_2O and pentane. The yield was 85%. ^{1}H NMR (300 MHz, 293 K, pyridine-d_5): δ (ppm) = 5.75(s, 8H, N_2S_2), 3.62(s, 4H, N_2S_2), 2.84(s, 2H, N_2S_2), 2.17(q, 2H, N_2S_2), 1.27(q, 2H, N_2S_2). ^{13}C NMR (300 MHz, 293 K, pyridine-d_5): δ (ppm) = 58.28, 53.01, 48.11, 24.23, 22.83. High Resolution $^+$ESI-Mass: $[M − Cl]^+$ ($C_9H_{18}InN_2S_2$) Calculated 332.9945; Found: 332.9939 (Most Abundant Isotopic Mass). The detailed isotope abundance is shown in Figure S6.

3.2. Reactions of XMN_2S_2 with Ni(II)

The white solid of XMN_2S_2 (0.1 mmol) was placed in a 50 mL flask, and 10 mL of a MeOH/MeCN (1:1) mixture was added. The green solution of $NiCl_2·6H_2O$ (0.1 mmol, 24 mg) in MeOH was then transferred to the 50 mL flask. The color immediately changed to maroon, which is typical of NiN_2S_2, and this product was confirmed by its X-ray structure. The same product, NiN_2S_2, was also formed by adding $Ni(BF_4)_2$ using the same method.

Similar to the reaction with the chloride salt of Ni^{II}, the white solid of XMN_2S_2 (0.1 mmol) was stirred with 10 mL MeCN in the 50 mL round flask. The NiP_2Cl_2 (P_2 = diphos or 1,1'-diphenylphosphinoethane, 0.105 g, 0.2 mmol) was dissolved in 10 mL MeCN and transferred to the flask. The resulting dark brown solution was dried in vacuo, giving a dark brown solid. Dark brown needle crystals were formed under Et_2O diffusion into a concentrated CH_3CN solution, proven to be the dinickel complex by X-ray structure and $^+$ESI-MS analyses.

3.3. Synthesis of $ClMW(CO)_5$

The $W(CO)_5$(solv) was generated in situ by $W(CO)_6$ in THF under UV light, after which the golden yellow solution was directly transferred to a white suspension of XMN_2S_2 (M = GaCl/InCl) in THF. Then, the mixture was stirred at room temperature and monitored by FTIR. After several hours, the color changed to a clear brown-orange and without further ν(CO) change. IR (cm^{-1}): $ClGaN_2S_2W(CO)_5$,

ν(CO) 2068(w), 1929(s), 1889(m); ClInN$_2$S$_2$W(CO)$_5$, ν(CO) 2068(w), 1929(s), 1892(m). $^-$ESI-Mass: [ClInN$_2$S$_2$W(CO)$_5$ + Cl]$^+$ (C$_{14}$H$_{18}$ClGaN$_2$O$_5$S$_2$W) Calculated 680.88; Found: 680.92; [ClInN$_2$S$_2$W(CO)$_5$ + Cl]$^+$ (C$_{14}$H$_{18}$ClInN$_2$O$_5$S$_2$W) Calculated 726.86; Found: 726.94.

4. Conclusions

Through this study, we have demonstrated that the main group metals Al, Ga, and In can bind within the tetradentate chelating pocket of an N$_2$S$_2$ ligand, yielding square pyramidal complexes. The M^{III} sits above the N$_2$S$_2$ plane and each is capped with an additional ligand, CH$_3^-$ in the case of Al^{III} and Cl$^-$ for Ga^{III} and In^{III}. Known to be tunable via the N to N and N to S linkers of the MN$_2$S$_2$ metallodithiolates, our account extends the range of metals that define the nucleophilicity of the sulfurs in metallodithiolates as aggregating sites for exogeneous metals. The system demonstrates that the XMN$_2$S$_2$ complexes bind to W(CO)$_5$ and W(CO)$_4$, forming isolable complexes, one of which was subjected to XRD analysis. Solution ν(CO) IR spectral values permit comparisons of donor ability with transition metals such as NiN$_2$S$_2$ where the Ni$_{d\pi}$–S$_{p\pi}$ antibonding interaction leads to greater donor ability. In addition, compared with NiN$_2$S$_2$, the XM^{III}N$_2$S$_2$ complexes are less stable and can readily convert to NiN$_2$S$_2$ on exposure to Ni^{II} when made available as a salt or when bound by diphos, bis-diphenylphosphino ethane. Such fundamental studies are useful for extending main group coordination chemistry.

Supplementary Materials: The following are available online at http://www.mdpi.com/2304-6740/7/9/115/s1: ^{1}H-NMR and ^{13}C-NMR Spectra (Figures S1–S3); Mass Spectra (Figures S4–S12); X-ray Crystal Structures (Figures S13–S16, Table S1–S4); FTIR Spectra of ClInN$_2$S$_2$·W(CO)$_4$ (Figure S17); The deviations of Nitrogen and Sulfur atoms from N$_2$S$_2$ plane (Figure S18); The ratio of M–N/M–S in XMN$_2$S$_2$ (Table S5); Different ν(CO) values in MW(CO)$_4$ comparison (Table S6).

Author Contributions: M.Y.D. and X.Y. designed the project. X.Y. synthesized and characterized the complexes. All authors contributed to the writing and editing the manuscript.

Conflicts of Interest: The authors declare no conflict of interest.

References

1. Busch, D.H.; Jicha, D.C.; Thompson, M.C.; Wrathall, J.W.; Blinn, E. Reactions of Coordinated Ligands. VIII. The Reactions of Alkyl Halides with Mercapto Groups in Transition Metal Complexes of Mercaptoamines. *J. Am. Chem. Soc.* **1964**, *86*, 3642–3650. [CrossRef]

2. Can, M.; Armstrong, F.A.; Ragsdale, S.W. Structure, Function, and Mechanism of the Nickel Metalloenzymes, CO Dehydrogenase, and Acetyl-CoA Synthase. *Chem. Rev.* **2014**, *114*, 4149–4174. [CrossRef] [PubMed]

3. Doukov, T.I.; Blasiak, L.C.; Seravalli, J.; Ragsdale, S.W.; Drennan, C.L. Xenon in and at the End of the Tunnel of Bifunctional Carbon Monoxide Dehydrogenase/Acetyl-CoA Synthase. *Biochemistry* **2008**, *47*, 3474–3483. [CrossRef] [PubMed]

4. Smee, J.J.; Miller, M.L.; Grapperhaus, C.A.; Reibenspies, J.H.; Darensbourg, M.Y. Subtle Bite-Angle Influences on N$_2$S$_2$Ni Complexes. *Inorg. Chem.* **2001**, *40*, 3601–3605. [CrossRef]

5. Mills, D.K.; Reibenspies, J.H.; Darensbourg, M.Y. Sterically protected nickel(II) in a N$_2$S$_2$ donor environment: 1,5-bis(mercaptoethyl)-1,5-diazacyclooctane and its methylated derivative. *Inorg. Chem.* **1990**, *29*, 4364–4366. [CrossRef]

6. Zhao, T.; Ghosh, P.; Martinez, Z.; Liu, X.; Meng, X.; Darensbourg, M.Y. Discrete Air-Stable Nickel(II)–Palladium(II) Complexes as Catalysts for Suzuki-Miyaura Reactions. *Organometallics* **2017**, *36*, 1822–1827. [CrossRef]

7. Denny, J.A.; Darensbourg, M.Y. Metallodithiolates as Ligands in Coordination, Bioinorganic, and Organometallic Chemistry. *Chem. Rev.* **2015**, *115*, 5248–5273. [CrossRef]

8. Yang, Z.; Yi, Y.; Zhong, M.; De, S.; Mondal, T.; Koley, D.; Ma, X.; Zhang, D.; Roesky, H.W. Addition Reactions of Me$_3$SiCN with Aldehydes Catalyzed by Aluminum Complexes Containing in Their Coordination Sphere O, S, and N Ligands. *Chem. Eur. J.* **2016**, *22*, 6932–6938. [CrossRef]

9. Chu, T.; Vyboishchikov, S.F.; Gabidullin, B.; Nikonov, G.I. Oxidative Cleavage of C=S and P=S Bonds at an Al^I Center: Preparation of Terminally Bound Aluminium Sulfides. *Angew. Chem. Int. Ed.* **2016**, *55*, 13306–13311. [CrossRef]

10. Kim, S.H.; Han, S.Y.; Kim, J.H.; Kang, Y.Y.; Lee, J.; Kim, Y. Monomeric or Dimeric Aluminium Complexes as Catalysts for Cycloaddition between CO$_2$ and Epoxides. *Eur. J. Inorg. Chem.* **2015**, *13*, 2323–2329. [CrossRef]

11. Darensbourg, D.J.; Billodeaux, D.R. Aluminum Salen Complexes and Tetrabutylammonium Salts: A Binary Catalytic System for Production of Polycarbonates from CO$_2$ and Cyclohexene Oxide. *Inorg. Chem.* **2005**, *44*, 1433–1442. [CrossRef] [PubMed]

12. Alam, I.S.; Arrowsmith, R.L.; Cortezon-Tamarit, F.; Twyman, F.; Kociok-Köhn, G.; Botchway, S.W.; Dilworth, J.R.; Carroll, L.; Aboagye, E.O.; Pascu, S.I. Microwave Gallium-68 Radiochemistry for Kinetically Stable bis(thiosemicarbazone) Complexes: Structural Investigations and Cellular Uptake under Hypoxia. *Dalton Trans.* **2015**, *45*, 144–155. [CrossRef] [PubMed]

13. Zhang, N.; Tai, Y.; Li, M.; Ma, P.; Zhao, J.; Niu, J. Main Group Bismuth(III), Gallium(III) and Diorganotin(IV) Complexes derived from bis(2-acetylpyrazine) thiocarbonohydrazone: Synthesis, Crystal Structures and Biological Evaluation. *Dalton Trans.* **2014**, *43*, 5182–5189. [CrossRef] [PubMed]

14. Zhang, W.; Dodonov, V.A.; Chen, W.; Zhao, Y.; Skatova, A.A.; Fedushkin, I.L.; Roesky, P.W.; Wu, B.; Yang, X.J. Cycloaddition versus Cleavage of the C=S Bond of Isothiocyanates Promoted by Digallane Compounds with Noninnocent α-Diimine Ligands. *Chem. Eur. J.* **2018**, *24*, 14994–15002. [CrossRef] [PubMed]

15. Tai, Y.; Ji, Y.; Lu, Y.; Li, M.; Wu, Y.; Han, Q. Cadmium(II) and Indium(III) Complexes Derived from 2-benzoylpyridine *N*(4)-cyclohexylthiosemicarbazone: Synthesis, Crystal Structures, Spectroscopic Characterization and Cytotoxicity. *Synth. Met.* **2016**, *219*, 109–114. [CrossRef]

16. Arrowsmith, R.L.; Waghorn, P.A.; Jones, M.W.; Bauman, A.; Brayshaw, S.K.; Hu, Z.; Kociok-Köhn, G.; Mindt, T.L.; Tyrrell, R.M.; Botchway, S.W.; et al. Fluorescent Gallium and Indium bis(thiosemicarbazonates) and Their Radiolabelled Analogues: Synthesis, Structures and Cellular Confocal Fluorescence Imaging Investigations. *Dalton Trans.* **2011**, *2011. 40*, 6238–6252. [CrossRef]

17. Anderson, T.S.; Briand, G.G.; Brüning, R.; Decken, A.; Margeson, M.J.; Pickard, H.M.; Trevors, E.E. Synthesis, Characterization and Reactivity of (dithiolato)Indium Complexes. *Polyhedron* **2017**, *135*, 101–108. [CrossRef]

18. Wadas, T.J.; Wong, E.H.; Weisman, G.R.; Anderson, C.J. Coordinating Radiometals of Copper, Gallium, Indium, Yttrium, and Zirconium for PET and SPECT Imaging of Disease. *Chem. Rev.* **2010**, *110*, 2858–2902. [CrossRef]

19. Addison, A.W.; Rao, T.N.; Reedijk, J.; Jacobus, V.R.; Verschoor, G.C. Synthesis, Structure, and Spectroscopic Properties of Copper(II) Compounds Containing Nitrogen–Sulphur Donor Ligands; the Crystal and Molecular Structure of aqua [1,7-bis(*N*-methylbenzimidazol-2′-yl)-2,6-dithiaheptane]Copper(II) Perchlorate. *J. Chem. Soc. Dalton Trans.* **1984**, *7*, 1349–1356. [CrossRef]

20. Hess, J.; Conder, H.L.; Green, K.N.; Darensbourg, M.Y. Electronic Effects of (N$_2$S$_2$)M(NO) Complexes (M = Fe, Co) as Metallodithiolate Ligands. *Inorg. Chem.* **2008**, *47*, 2056–2063. [CrossRef]

21. Jenkins, R.; Pinder, T.A.; Hatley, M.L.; Reibenspies, J.H.; Darensbourg, M.Y. Tetradentate N$_2$S$_2$ Vanadyl(IV) Coordination Complexes: Synthesis, Characterization, and Reactivity Studies. *Inorg. Chem.* **2011**, *50*, 1849–1855. [CrossRef] [PubMed]

22. Darensbourg, D.J.; Kump, R.L. A Convenient Synthesis of *cis*-Mo(CO)$_4$L$_2$ Derivatives (L = Group 5A Ligand) and a Qualitative Study of Their Thermal Reactivity toward Ligand Dissociation. *Inorg. Chem.* **1978**, *17*, 2680–2682. [CrossRef]

23. Rampersad, M.V.; Jeffery, S.P.; Golden, M.L.; Lee, J.; Reibenspies, J.H.; Darensbourg, D.J.; Darensbourg, M.Y. Characterization of Steric and Electronic Properties of NiN$_2$S$_2$ Complexes as S-donor Metallodithiolate Ligands. *J. Am. Chem. Soc.* **2005**, *127*, 17323–17334. [CrossRef] [PubMed]